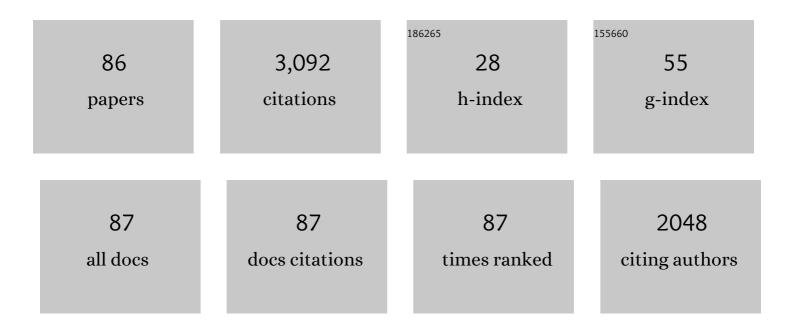
Andrew Jirasek

List of Publications by Year in descending order

Source: https://exaly.com/author-pdf/7585207/publications.pdf Version: 2024-02-01



#	Article	IF	CITATIONS
1	Group and Basis Restricted Non-Negative Matrix Factorization and Random Forest for Molecular Histotype Classification and Raman Biomarker Monitoring in Breast Cancer. Applied Spectroscopy, 2022, 76, 462-474.	2.2	9
2	Superiorization versus regularization: A comparison of algorithms for solving image reconstruction problems with applications in computed tomography. Medical Physics, 2022, 49, 1065-1082.	3.0	4
3	Simulated design optimization of a prototype solid tank optical CT scanner for 3D radiation dosimetry. Journal of Physics: Conference Series, 2022, 2167, 012009.	0.4	0
4	Raman spectroscopy and group and basis-restricted non negative matrix factorisation identifies radiation induced metabolic changes in human cancer cells. Scientific Reports, 2021, 11, 3853.	3.3	16
5	A Methodology for Dynamic Material Characterizations via Terahertz Time-Domain Spectroscopy. IEEE Transactions on Terahertz Science and Technology, 2020, 10, 282-291.	3.1	3
6	Monitor Ionizing Radiation-Induced Cellular Responses with Raman Spectroscopy, Non-Negative Matrix Factorization, and Non-Negative Least Squares. Applied Spectroscopy, 2020, 74, 701-711.	2.2	14
7	Linac-integrated kV-cone beam CT polymer gel dosimetry. Physics in Medicine and Biology, 2020, 65, 225030.	3.0	7
8	Evaluation of an x-ray CT polymer gel dosimetry system in the measurement of deformed dose. Biomedical Physics and Engineering Express, 2020, 6, 035031.	1.2	8
9	Optimization of solid tank design for fan-beam optical CT based 3D radiation dosimetry. Physics in Medicine and Biology, 2020, 65, 245012.	3.0	7
10	Raman spectroscopy detects metabolic signatures of radiation response and hypoxic fluctuations in non-small cell lung cancer. BMC Cancer, 2019, 19, 474.	2.6	9
11	Delivered Dose Distribution Visualized Directly With Onboard kV-CBCT: Proof of Principle. International Journal of Radiation Oncology Biology Physics, 2019, 103, 1271-1279.	0.8	22
12	Haralick texture feature analysis for quantifying radiation response heterogeneity in murine models observed using Raman spectroscopic mapping. PLoS ONE, 2019, 14, e0212225.	2.5	11
13	Introduction of a deformable x-ray CT polymer gel dosimetry system. Physics in Medicine and Biology, 2018, 63, 075014.	3.0	14
14	<i>Ex Vivo</i> Detection of Circulating Tumor Cells from Whole Blood by Direct Nanoparticle Visualization. ACS Nano, 2018, 12, 1902-1909.	14.6	30
15	Raman Spectroscopic Signatures Reveal Distinct Biochemical and Temporal Changes in Irradiated Human Breast Adenocarcinoma Xenografts. Radiation Research, 2018, 189, 497.	1.5	19
16	Characteristics of a Ce-Doped silica fiber irradiated by 74†MeV protons. Radiation Measurements, 2018, 114, 19-24.	1.4	11
17	Breast cancer subtype specific biochemical responses to radiation. Analyst, The, 2018, 143, 3850-3858.	3.5	18
18	Plasmonic labeling of subcellular compartments in cancer cells: multiplexing with fine-tuned gold and silver nanoshells. Chemical Science, 2017, 8, 3038-3046.	7.4	27

#	Article	IF	CITATIONS
19	Improving the quality of reconstructed X-ray CT images of polymer gel dosimeters: zero-scan coupled with adaptive mean filtering. Australasian Physical and Engineering Sciences in Medicine, 2017, 40, 159-165.	1.3	7
20	Evaluation of accuracy and precision in polymer gel dosimetry. Medical Physics, 2017, 44, 736-746.	3.0	19
21	Optical and X-ray computed tomography scanning of 3D dosimeters. Journal of Physics: Conference Series, 2017, 847, 012019.	0.4	3
22	Accuracy and reproducibility in x-ray computed tomography polymer gel dosimetry. Journal of Physics: Conference Series, 2017, 847, 012047.	0.4	0
23	Design and application of 3D-printed stepless beam modulators in proton therapy. Physics in Medicine and Biology, 2016, 61, N276-N290.	3.0	9
24	Raman spectroscopy identifies radiation response in human non-small cell lung cancer xenografts. Scientific Reports, 2016, 6, 21006.	3.3	57
25	A Raman Spectroscopic Study of Cell Response to Clinical Doses of Ionizing Radiation. Applied Spectroscopy, 2015, 69, 193-204.	2.2	46
26	Incorporating multislice imaging into xâ€ray CT polymer gel dosimetry. Medical Physics, 2015, 42, 1666-1677.	3.0	10
27	Assessment of the effects of CT dose in averaged x-ray CT images of a dose-sensitive polymer gel. Journal of Physics: Conference Series, 2015, 573, 012075.	0.4	1
28	Radiation-Induced Glycogen Accumulation Detected by Single Cell Raman Spectroscopy Is Associated with Radioresistance that Can Be Reversed by Metformin. PLoS ONE, 2015, 10, e0135356.	2.5	28
29	3D printed plastics for beam modulation in proton therapy. Physics in Medicine and Biology, 2015, 60, N231-N240.	3.0	20
30	Dose rate properties of NIPAM-based x-ray CT polymer gel dosimeters. Physics in Medicine and Biology, 2015, 60, 4399-4411.	3.0	11
31	Uncertainty in 3D gel dosimetry. Journal of Physics: Conference Series, 2015, 573, 012008.	0.4	18
32	Radiationâ€induced refraction artifacts in the optical CT readout of polymer gel dosimeters. Medical Physics, 2014, 41, 112102.	3.0	5
33	Dose calibration optimization and error propagation in polymer gel dosimetry. Physics in Medicine and Biology, 2014, 59, 597-614.	3.0	20
34	Sci-Fri AM: Mountain - 04: Label-free Raman spectroscopy of single tumour cells detects early radiation-induced glycogen synthesis associated with increased radiation resistance. Medical Physics, 2014, 41, 23-24.	3.0	0
35	Characterization of the essential dosimetric properties of cosolvent-free polymer gel dosimeters: Recent progress in x-ray CT based normoxic polymer gel dosimetry. Journal of Physics: Conference Series, 2013, 444, 012092.	0.4	0
36	Considerations for x-ray CT polymer gel dosimetry. Journal of Physics: Conference Series, 2013, 444, 012005.	0.4	5

#	Article	IF	CITATIONS
37	Statistical Correlation Between SERS Intensity and Nanoparticle Cluster Size. Journal of Physical Chemistry C, 2013, 117, 16596-16605.	3.1	41
38	Revealing the impact of radiation-induced refractive index changes in polymer gel dosimeters. Journal of Physics: Conference Series, 2013, 444, 012077.	0.4	0
39	Recent developments with a prototype fan-beam optical CT scanner. Journal of Physics: Conference Series, 2013, 444, 012066.	0.4	1
40	A prototype fanâ€beam optical CT scanner for 3D dosimetry. Medical Physics, 2013, 40, 061712.	3.0	27
41	An x-ray CT polymer gel dosimetry prototype: I. Remnant artefact removal. Physics in Medicine and Biology, 2012, 57, 3137-3153.	3.0	30
42	An x-ray CT polymer gel dosimetry prototype: II. Gel characterization and clinical application. Physics in Medicine and Biology, 2012, 57, 3155-3175.	3.0	44
43	Raman spectroscopy of single human tumour cells exposed to ionizing radiation <i>in vitro</i> . Physics in Medicine and Biology, 2011, 56, 19-38.	3.0	52
44	Biochemical signatures of <i>in vitro</i> radiation response in human lung, breast and prostate tumour cells observed with Raman spectroscopy. Physics in Medicine and Biology, 2011, 56, 6839-6855.	3.0	58
45	Cosolvent-free polymer gel dosimeters with improved dose sensitivity and resolution for x-ray CT dose response. Physics in Medicine and Biology, 2011, 56, 2091-2102.	3.0	58
46	SU-E-T-93: A CT Polymer Gel Dosimetry System for End-To-End Dosimetry. Medical Physics, 2011, 38, 3507-3507.	3.0	8
47	Alternative imaging modalities for polymer gel dosimetry. Journal of Physics: Conference Series, 2010, 250, 012070.	0.4	4
48	Preliminary investigations with a photodiode-based fan-beam optical CT scanner. Journal of Physics: Conference Series, 2010, 250, 012024.	0.4	3
49	Isopropanol-based polymer gel dosimeters for use with x-ray CT imaging. Journal of Physics: Conference Series, 2010, 250, 012072.	0.4	3
50	Polymer gel dosimetry. Physics in Medicine and Biology, 2010, 55, R1-R63.	3.0	755
51	Variability in Raman Spectra of Single Human Tumor Cells Cultured <i>in vitro</i> : Correlation with Cell Cycle and Culture Confluency. Applied Spectroscopy, 2010, 64, 871-887.	2.2	99
52	A Matrix-Based Two-Dimensional Regularization Algorithm for Signal-to-Noise Ratio Enhancement of Multidimensional Spectral Data. Applied Spectroscopy, 2010, 64, 1209-1219.	2.2	7
53	Polymer gel dosimeters with enhanced sensitivity for use in x-ray CT polymer gel dosimetry. Physics in Medicine and Biology, 2010, 55, 5269-5281.	3.0	76
54	How does the chemistry of polymer gel dosimeters affect their performance?. Journal of Physics: Conference Series, 2009, 164, 012003.	0.4	8

#	Article	IF	CITATIONS
55	Preliminary investigation of the NMR, optical and x-ray CT dose-response of polymer gel dosimeters with cosolvents and increased crosslinker levels. Journal of Physics: Conference Series, 2009, 164, 012017.	0.4	2
56	Preliminary investigation of the NMR, optical and x-ray CT dose–response of polymer gel dosimeters incorporating cosolvents to improve dose sensitivity. Physics in Medicine and Biology, 2009, 54, 2779-2790.	3.0	58
57	Effects of glycerol co-solvent on the rate and form of polymer gel dose response. Physics in Medicine and Biology, 2009, 54, 907-918.	3.0	26
58	The Use of Ultraviolet Resonance Raman Spectroscopy in the Analysis of Ionizing-Radiation-Induced Damage in DNA. Applied Spectroscopy, 2009, 63, 412-422.	2.2	11
59	An overview of polymer gel dosimetry using x-ray CT. Journal of Physics: Conference Series, 2009, 164, 012038.	0.4	8
60	A prototype fan-beam optical CT scanner for polymer gel dosimetry. Journal of Physics: Conference Series, 2009, 164, 012025.	0.4	5
61	Adaptive mean filtering for noise reduction in CT polymer gel dosimetry. Medical Physics, 2008, 35, 344-355.	3.0	42
62	Investigation of a two-point maximum entropy regularization method for signal enhancement applied to magnetoencephalography data. Biomedical Signal Processing and Control, 2008, 3, 78-87.	5.7	3
63	Two-Point Maximum Entropy Noise Discrimination in Spectra over a Range of Baseline Offsets and Signal-to-Noise Ratios. Applied Spectroscopy, 2007, 61, 157-164.	2.2	11
64	MEG signal enhancement using a two-point maximum entropy regularization method. International Congress Series, 2007, 1300, 241-244.	0.2	1
65	Xâ€ r ay CT dose in normoxic polyacrylamide gel dosimetry. Medical Physics, 2007, 34, 1934-1943.	3.0	30
66	Investigation of X-ray CT dose in normoxic polyacrylamide gel dosimetry. , 2007, , 1873-1876.		0
67	Investigation of tetrakis hydroxymethyl phosphonium chloride as an antioxidant for use in x-ray computed tomography polyacrylamide gel dosimetry. Physics in Medicine and Biology, 2006, 51, 1891-1906.	3.0	75
68	Experimental investigations of polymer gel dosimeters. Journal of Physics: Conference Series, 2006, 56, 23-34.	0.4	20
69	Experimental properties of THPC based normoxic polyacrylamide gels for use in x-ray computed tomography gel dosimetry. Journal of Physics: Conference Series, 2006, 56, 263-267.	0.4	4
70	Discrimination between UV radiation-induced and thermally induced spectral changes in AT-paired DNA oligomers using UV resonance Raman spectroscopy. Journal of Raman Spectroscopy, 2006, 37, 1368-1380.	2.5	24
71	Investigation of a 2D two-point maximum entropy regularization method for signal-to-noise ratio enhancement: application to CT polymer gel dosimetry. Physics in Medicine and Biology, 2006, 51, 2599-2617.	3.0	30
72	Assessment of CT dose in X-ray CT polyacrylamide gel dosimetry. Journal of Physics: Conference Series, 2006, 56, 268-271.	0.4	0

#	Article	IF	CITATIONS
73	Technical considerations for implementation of x-ray CT polymer gel dosimetry. Physics in Medicine and Biology, 2005, 50, 1727-1745.	3.0	63
74	Spectroscopic Studies of the Anaerobic Enzymeâ^'Substrate Complex of Catechol 1,2-Dioxygenase. Journal of the American Chemical Society, 2005, 127, 16882-16891.	13.7	39
75	Investigation of Selected Baseline Removal Techniques as Candidates for Automated Implementation. Applied Spectroscopy, 2005, 59, 545-574.	2.2	284
76	Effects of gel composition on the radiation induced density change in PAG polymer gel dosimeters: a model and experimental investigations. Physics in Medicine and Biology, 2004, 49, 2477-2490.	3.0	50
77	Accuracy and Precision of Manual Baseline Determination. Applied Spectroscopy, 2004, 58, 1488-1499.	2.2	73
78	The response of PAG density to dose: a model and experimental investigations. Journal of Physics: Conference Series, 2004, 3, 163-167.	0.4	2
79	Revealing System Dynamics through Decomposition of the Perturbation Domain in Two-Dimensional Correlation Spectroscopy. Applied Spectroscopy, 2003, 57, 1551-1560.	2.2	13
80	Identification and Interpretation of Generalized Two-Dimensional Correlation Spectroscopy Features through Decomposition of the Perturbation Domain. Applied Spectroscopy, 2003, 57, 1561-1574.	2.2	19
81	Relative effectiveness of polyacrylamide gel dosimeters applied to proton beams: Fourier transform Raman observations and track structure calculations. Medical Physics, 2002, 29, 569-577.	3.0	51
82	CT gel dosimetry technique: Comparison of a planned and measured 3D stereotactic dose volume. Journal of Applied Clinical Medical Physics, 2002, 3, 110-118.	1.9	26
83	CT gel dosimetry technique: Comparison of a planned and measured 3D stereotactic dose volume. Journal of Applied Clinical Medical Physics, 2002, 3, 110.	1.9	50
84	Effects of crosslinker fraction in polymer gel dosimeters using FT Raman spectroscopy. Physics in Medicine and Biology, 2001, 46, 1949-1961.	3.0	44
85	Characterization of monomer/crosslinker consumption and polymer formation observed in FT-Raman spectra of irradiated polyacrylamide gels. Physics in Medicine and Biology, 2001, 46, 151-165.	3.0	71
86	Polymer gel dosimetry using x-ray computed tomography: a feasibility study4. Physics in Medicine and Biology, 2000, 45, 2559-2571.	3.0	195